



Review

Off-Resonance Control and All-Optical Switching: Expanded Dimensions in Nonlinear Optics

David S. Bradshaw , Kayn A. Forbes  and David L. Andrews *School of Chemistry, University of East Anglia, Norwich Research Park, Norwich NR4 7TJ, UK;
d.bradshaw@uea.ac.uk (D.S.B.); k.forbes@uea.ac.uk (K.A.F.)

* Correspondence: d.l.andrews@uea.ac.uk

Received: 6 September 2019; Accepted: 8 October 2019; Published: 11 October 2019



Abstract: The theory of non-resonant optical processes with intrinsic optical nonlinearity, such as harmonic generation, has been widely understood since the advent of the laser. In general, such effects involve multiphoton interactions that change the population of each input optical mode or modes. However, nonlinear effects can also arise through the input of an off-resonant laser beam that itself emerges unchanged. Many such effects have been largely overlooked. Using a quantum electrodynamical framework, this review provides detail on such optically nonlinear mechanisms that allow for a controlled increase or decrease in the intensity of linear absorption and fluorescence and in the efficiency of resonance energy transfer. The rate modifications responsible for these effects were achieved by the simultaneous application of an off-resonant beam with a moderate intensity, acting in a sense as an optical catalyst, conferring a new dimension of optical nonlinearity upon photoactive materials. It is shown that, in certain configurations, these mechanisms provide the basis for all-optical switching, i.e., the control of light-by-light, including an optical transistor scheme. The conclusion outlines other recently proposed all-optical switching systems.

Keywords: nonlinear optics; all-optical switch; absorption; fluorescence; resonance energy transfer; FRET; second harmonic generation; laser action; optical transistor; multiphoton process

1. Introduction

Nonlinear optics is one of the most remarkable and pervasive fields to emerge from the development of the laser over 50 years ago. Optically parametric processes, such as second and third harmonic generation (SHG and THG), are the preeminent means of converting laser output to a shorter wavelength. The basic theoretical principles of nonlinear optics were rapidly established and consolidated, notably in an early treatise by Bloembergen in 1965 [1]. More modern introductions to the field include prominent texts by Jha [2], Sauter [3], He and Liu [4], Shen [5], Sutherland [6], Banerjee [7], Novotny, Hecht [8], and Boyd [9], among many others.

Conventionally, nonlinear processes involve the concurrent absorption of multiple off-resonant photons—meaning that the associated rate depends on the square, or a higher order, of the corresponding input laser intensity. In resonant processes, this typically produces local dipole transitions to a higher energy (most often electronically excited) state. In non-resonant parametric processes, each fundamental interaction results in the promotion of the active material to a virtual intermediate state, which then returns to the ground state via emission into an optical mode or modes that differs, usually in frequency, from the laser input.

Largely overlooked is the fact that a moderately intense off-resonant laser beam ($\sim 10^{11}$ – 10^{12} W cm⁻²) may provide a controlling effect on a resonant process such as fluorescence—acting as a stimulus with an optical frequency at which the molecule is transparent. In such a case, the beam is unaltered by the light-matter interactions that occur. To this extent, ‘optical catalyst’ is an

apt name for the effect, since the beam is unchanged before and after the process. The term is also used in a different connection relating to beam splitting. Here, optical catalysts have been extensively studied [10–13] and suggested as a method for improved performance of continuous-variable quantum key distribution systems [14]. Moreover, in connection to the photolysis of isolated phenol molecules, a strong off-resonant infrared electromagnetic field has recently been shown to lower the activation barrier to photolysis via a dynamic Stark shift [15], signifying a form of optical catalysis whose effect is also analogous to those detailed in this review.

Applying the off-resonant beam to a conventional optically resonant process results in an unconventional nonlinear optical effect. The outcome is the possibility of an increased or decreased rate compared to the resonant process without the ancillary beam. The capacity for the stimulus beam to be under direct experimental control confers numerous advantages, especially compared with the commonly known capacity of a neighboring surface plasmon to enhance the rate of many optical processes [16–41]. Moreover, if the resonant process is forbidden by virtue of selection rules or another symmetry constraint, it is possible that it can become entirely activated by the input beam, since the resultant nonlinear process may then be allowed. This is the potential basis for an all-optical switch. Here, the realm of application may extend to control circuitry in signal propagation and waveguide networks for optical communication [42].

In this review, we first recap on the formulation for conventional nonlinear optics, serving to introduce a quantum electrodynamical framework that is equally valid for the newer effects that will be our focus. The approach is concisely illustrated for the process of second harmonic generation (Section 2). Sections 3 and 4 provide an analysis of the effect of an off-resonant beam on absorption and fluorescence. These processes are known as laser-modified absorption and fluorescence. It is important to note that these differ from standard nonlinear optics, in that the laser-modified processes involve a resonant mode along with the off-resonant beam. Section 5 delivers an overview of optically controlled resonance energy transfer, which may be interpreted as optical catalysis of energy transfer. It is shown that this effect has a fundamental connection to the well-established phenomenon of optical binding, which also involves an off-resonant input beam. The penultimate Section introduces the potential for all-optical switching based on each mechanism and entertains the possibility of an optical transistor in a related scheme. The concluding section provides a discussion of the context for deploying these and other schemes for all-optical switching.

2. Conventional Nonlinear Optics

From the viewpoint of quantum electrodynamics (QED) [43,44], all optical interactions occur through the annihilation and creation of photons. A central motivation to utilizing the quantized radiation field over classical wave theory is the ability to account for the spontaneous generation of new modes of light [45]. This has obvious significance in the field of nonlinear optics, where new modes of light are invariably produced in processes such as harmonic generation and hyper-Raman scattering. One principle flaw of using classical wave theory to describe specific nonlinear processes is that it suggests the ability of generating a second harmonic even at the intensity level of a single photon. Moreover, for spectroscopic interactions involving quantum transitions, the interplay of energetics and selection rules based on angular momentum can be understood in no other satisfactory way. Within the realm of nonlinear optics, there are numerous further reasons why a photon-based description of nonlinear optical phenomena is advisable over the classical wave picture of light (described elsewhere [45–47]). For all these reasons, casting light-matter interactions in QED offers the best route to take in this review to fully develop and describe the mechanisms of nonlinear optical interaction.

The most suitable Hamiltonian to describe non-relativistic light-matter interactions is the fully quantized Power-Zienau-Woolley (PZW) multipolar Hamiltonian [48]. Its merits include gauge-independence, its optical elements being directly cast in terms of electromagnetic fields only, casting the interactions between light and matter through a Hamiltonian operator H_{int} as couplings

between the electromagnetic fields and the multipolar transition moments of the material component. Furthermore, all electrostatic interactions are mediated by transverse photons, i.e., they are intrinsically causal and fully retarded. In the dipole-approximation, H_{int} takes the form

$$H_{\text{int}} = -\epsilon_0 \sum_{\xi} \mu_i(\xi) d_i^{\perp}(\mathbf{R}_{\xi}) \tag{1}$$

where for a molecule ξ positioned at \mathbf{R}_{ξ} , $\mu(\xi)$ is the electric-dipole transition moment operator and $d^{\perp}(\mathbf{R}_{\xi})$ the electric-displacement field operator: The interaction (1) represents the E1 (electric-dipole) interaction with the field. Throughout this work, we invoke standard subscript notation, i.e., summation over indices is implied, such that in Equation (1):

$$\sum_{i=x,y,z} \mu_i d_i^{\perp} = \mu_x d_x^{\perp} + \mu_y d_y^{\perp} + \mu_z d_z^{\perp} = \boldsymbol{\mu} \cdot \mathbf{d}^{\perp} \tag{2}$$

The electric-displacement field operator has a standard mode expansion for which each mode includes two terms: One for a photon annihilation and the other for a photon creation [43]. The explicit form of the mode expansion is written as

$$\mathbf{d}^{\perp}(\mathbf{R}_{\xi}) = i \left(\frac{\hbar c k \epsilon_0}{2V} \right)^{\frac{1}{2}} \left\{ e \mathbf{a} e^{i\mathbf{k} \cdot \mathbf{R}_{\xi}} - \bar{e} \mathbf{a}^{\dagger} e^{-i\mathbf{k} \cdot \mathbf{R}_{\xi}} \right\} \tag{3}$$

where $\hbar c k$ and e are the energy and unit polarization vector of a given photon, respectively, and the overbar denotes its complex conjugate. Moreover, V is the quantization volume, a and a^{\dagger} are the annihilation and creation operators, respectively, and the phase factors are represented by $e^{i\mathbf{k} \cdot \mathbf{R}_{\xi}}$.

The time evolution of the system is determined by the Schrödinger equation, approximate solutions of which are commonly secured with the use of time-dependent perturbation theory [49]. For optical interactions, the energies associated with the interaction Hamiltonian (1) are much smaller in magnitude than those represented by the matter, typically written for a molecule as H_{mol} and radiation (H_{rad}) Hamiltonians. Light-molecule interactions, through the H_{int} operator, may thus be seen to effect perturbations on the eigenstates of $H_{\text{mol}} + H_{\text{rad}}$ and, therefore, lead to transitions between system states. Although the term ‘transition’ is usually applied to material quantum state transitions, here it equally applies to changes in the populations of radiation states. The matrix element (or quantum amplitude) may thus be expanded in powers of the perturbation operator:

$$M_{fi} = \langle f | H_{\text{int}} | i \rangle + \sum_r \frac{\langle f | H_{\text{int}} | r \rangle \langle r | H_{\text{int}} | i \rangle}{E_i - E_r} + \sum_{r,s} \frac{\langle f | H_{\text{int}} | s \rangle \langle s | H_{\text{int}} | r \rangle \langle r | H_{\text{int}} | i \rangle}{(E_i - E_r)(E_i - E_s)} + \sum_{r,s,t} \frac{\langle f | H_{\text{int}} | t \rangle \langle t | H_{\text{int}} | s \rangle \langle s | H_{\text{int}} | r \rangle \langle r | H_{\text{int}} | i \rangle}{(E_i - E_t)(E_i - E_s)(E_i - E_r)} + \dots \tag{4}$$

where r , s , and t are the virtual intermediate system states and E in the energy of the state denoted by its subscript. Through $\mathbf{d}^{\perp}(\mathbf{R}_{\xi})$, H_{int} applies to one photon-molecule interaction, meaning that the first term of Equation (4) relates to one photon-molecule interaction, the second term corresponds to two interactions, etc.

Before proceeding further, it is worth commenting on issues that will be the later focus of this review. Successive terms in the above series are commonly associated with diminishing levels of effect, such that the leading non-vanishing term contributing to any given effect is the one whose order equates to the number of photons involved, per interaction. This may seem obvious: It follows from the linear dependence of H_{int} on the electric displacement field through Equation (1), and the linear dependence that the field operator itself has on photon annihilation and creation operators. So, for example, the theory of single-photon absorption is routinely cast in terms of the leading term in Equation (4). The next lowest order of perturbation theory that may contribute is the third order, physically corresponding to the absorption of two photons coupled with the stimulated emission of

one photon back into the same optical mode (classically, one would recognize this as arising from $\cos \omega t$ term in the identity $(\cos \omega t)^3 = \frac{1}{4}(\cos \omega t + \cos 3\omega t)$.) However, such contributions would normally be associated with a cubic dependence on the electric field strength, rendering the effect comparatively insignificant at any intensity below the ultra-high intensity level at which both perturbation theory and molecules themselves break down. In the next section, we demonstrate how the involvement of two throughput beams dramatically changes the significance of the third-order term.

First, to briefly provide an indicative example of the use of QED for conventional *nonlinear* optics, we derive the quantum amplitude and corresponding rate and radiant intensity of SHG. Second harmonic generation is a frequency-doubling, three-photon process, fundamentally involving the pairwise annihilation of input photons of frequency ω (wave-vector \mathbf{k} and polarization η) correlated with the creation of single photons of frequency 2ω (\mathbf{k}' , η'). The coherent, linear momentum-conserving process dictates the relationship $2\mathbf{k} = \mathbf{k}'$ between the input photons and output photon wave-vector. The matrix element is obtained using third-order perturbation theory, corresponding to the third term of Equation (4), where the initial state expressed in Dirac ket notation is $|i_{\text{mol}}; i_{\text{rad}}\rangle = |E_0; n(\mathbf{k}, \eta)\rangle$, and the final state is $|f_{\text{mol}}; f_{\text{rad}}\rangle = |E_0; (n-2)(\mathbf{k}, \eta), 1(\mathbf{k}', \eta')\rangle$. Inserting Equation (1) into the third term of Equation (4), and working through the detailed analysis, delivers the matrix element

$$M_{fi} = -\frac{i}{2} \left(\frac{\hbar c k}{\epsilon_0 V} \right)^{\frac{3}{2}} \{n(n-1)\}^{\frac{1}{2}} \bar{e}'_i e_j e_k \sum_{\xi} \beta_{ijk}^{(\xi)}(-2\omega; \omega, \omega) \tag{5}$$

where, in this specific case, e and e' are unit polarization vectors of the incident and emitted photons, respectively. The molecule-level response is denoted by β_{ijk} , the frequency-dependent hyperpolarizability tensor

$$\beta_{ijk}(-2\omega; \omega, \omega) = \frac{1}{2} \sum_{r,s} \left[\left\{ \frac{\mu_i^{0s} \mu_j^{sr} \mu_k^{r0}}{(E_0 - E_s + 2\hbar\omega)(E_0 - E_r + \hbar\omega)} + \frac{\mu_j^{0s} \mu_i^{sr} \mu_k^{r0}}{(E_0 - E_s - \hbar\omega)(E_0 - E_r + \hbar\omega)} \right. \right. \\ \left. \left. + \frac{\mu_j^{0r} \mu_k^{rs} \mu_i^{s0}}{(E_0 - E_s - \hbar\omega)(E_0 - E_r - 2\hbar\omega)} + \{j \leftrightarrow k\} \right\} \right]. \tag{6}$$

The rate of SHG for a collection of N molecules is determined from the Fermi rate rule $\Gamma = 2\pi\hbar^{-1} \rho_f |M_{fi}|^2$, where ρ_f is the density of final states for the radiation. In terms of the second harmonic radiant intensity I , we find the result

$$2\hbar c k \frac{d\Gamma}{d\Omega} = I = \frac{\bar{I}_0^2 g^{(2)} k^4 N^2}{2\pi^2 \epsilon_0^3 c} \left| \bar{e}'_i e_j e_k \left\langle \beta_{ijk}^{(\xi)}(-2\omega; \omega, \omega) \right\rangle \right|^2 \tag{7}$$

where \bar{I}_0 is the mean irradiance of the input beam (note its quadratic dependence), $g^{(2)}$ is the degree of second order coherence, and angular brackets denote the rotational averaging required only if the sample is a structureless fluid or an isotropic solid. The average of the third-rank hyperpolarizability tensor is then $\langle \beta_{ijk} \rangle \approx \epsilon_{ijk} \epsilon_{\lambda\mu\nu} \beta_{\lambda\mu\nu}$, which produces $\epsilon_{ijk} \bar{e}'_i e_j e_k = 0$ on account of contracting the totally antisymmetric isotropic third-rank Levi-Civita tensor ϵ_{ijk} with the j, k -symmetric polarization component product. Hence, we secure the well-known result that SHG (and indeed all even-harmonic generation) is forbidden in randomly oriented or isotropic samples. In all other cases, the result is readily rewritten in terms of corresponding bulk quantities. Here, the latter implies the use of the second-order optical susceptibility, $\chi(-2\omega, \omega, \omega)$. Second harmonic generation is the simplest nonlinear optical process, and the methods briefly outlined here form the basis of the analysis that follows [50].

3. Laser-Modified Absorption

In conventional ultraviolet/visible spectroscopy, resonant absorption occurs as molecules are promoted to allowed electronic excited states, and the resulting absorption spectrum represents an identifying characteristic of the molecular orbital structures [51]. It transpires that simultaneously

passing fixed-frequency, off-resonant laser light through the sample in the course of such absorption measurements may enhance or suppress the efficiency of light absorption differentially in each absorption band [52]. This concurrent process is shown in Figure 1. As we have seen, conventional absorption involves a single photon-molecule interaction that corresponds to the first term of Equation (4). Subjecting the absorbing system to the off-resonant laser beam provides for the additional involvement of three-photon-molecule couplings, as shown in Figure 2a, involving the third term of Equation (4). Although this is a higher order term, its contribution to the process need not be insignificant compared to the one for single-photon absorption. The off-resonant beam is independent of the resonant beam and, at sufficient intensity, it may exert a comparatively substantial influence even when the resonant beam is no more intense than is common in absorption spectroscopy. For the laser-modified process, the resonant absorption couples with elastic forward-scattering of the off-resonant beam, the latter itself delivering no net absorption or emission: Off-resonant photons are annihilated and created back into the same radiation mode that, therefore, emerges unchanged.

Before going further, it is important to stress that the selection rules for any three-quantum dipole transition invariably subsume those for a single-quantum transition, provided that the optical input and/or output comprises linear polarizations. The converse is, of course, not universally true, being dependent upon the relative symmetry properties of the associated ground and excited states in each case. Therefore, when off-resonant radiation becomes involved through a three-quantum transition in a single-photon absorption process, the result is that transition strengths for each absorption band may be significantly and individually modified. As we demonstrate, new bands satisfying only three-quantum selection rules may also appear when the off-resonant beam is sufficiently intense.

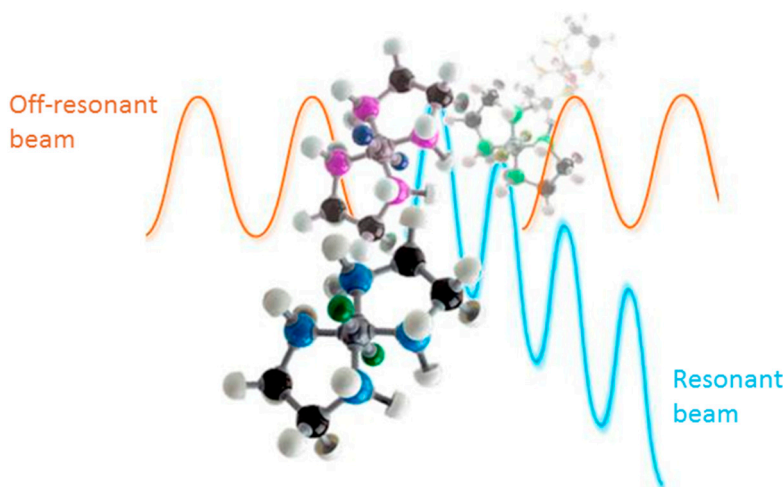


Figure 1. Depiction of a laser-modified absorption process.

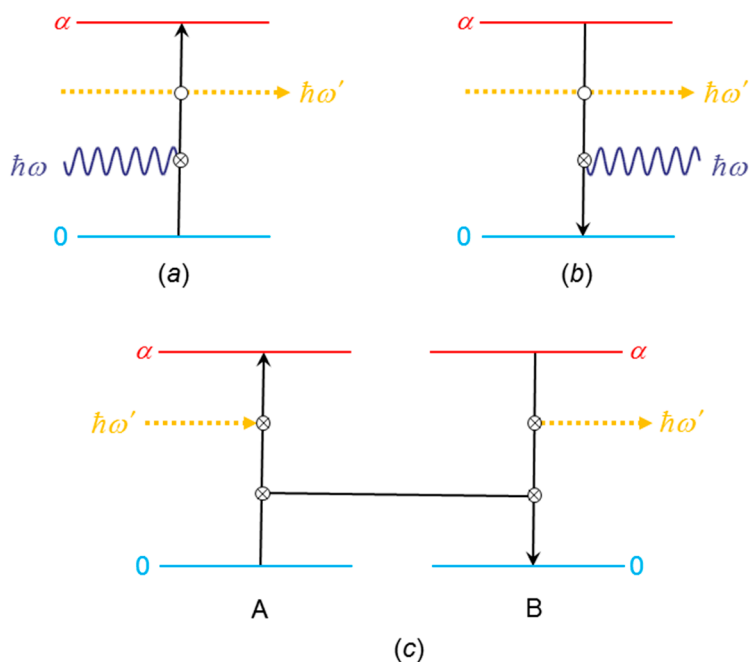


Figure 2. Energy-level diagrams for (a) laser-modified absorption, (b) laser-modified fluorescence and (c) optically controlled resonance energy transfer. Light blue and red horizontal lines denote ground-state 0 and excited-state α energy levels of the molecules, respectively, orange dashed lines represent the off-resonant beam, $\hbar\omega'$, and blue wavy lines are the resonant beam, $\hbar\omega$. Crossed and open circles are one- and two-photon interactions, respectively, the vertical black arrows denote electronic transitions and horizontal black line signifies energy transfer from A to B. Without the off-resonant beam, these diagrams simply depict absorption, fluorescence, and energy transfer. The beam that is applied concurrently (not step-wise) to these processes, as a result, suffers the annihilation and creation of one photon into the same radiation mode via virtual intermediate states (not shown). These depictions avoid the complexities of Feynman diagrams, or state-sequence diagrams, that show the whole range of interaction sequences necessarily involved [52–54].

The rate of laser-modified absorption, if no other mechanism were to be allowed, has a purely quadratic dependence on the intensity of the off-resonant beam. We return to the significance of this possibility under special conditions in Section 6. More commonly, however, the rate equation also includes a term representing a larger contribution to the total rate. This relates to the cross term (quantum interference) of the quantum amplitudes for conventional and laser-modified one-photon absorption. This is determined from the Fermi rate expression as $\Gamma_{\text{abs}} \sim |M_{fi}^{(1)} + M_{fi}^{(3)}|^2$, where $M_{fi}^{(1)}$ and $M_{fi}^{(3)}$ are the quantum amplitudes for the leading first-order (single-photon) and third-order (laser-modified) interaction processes, respectively. The interference effects depend on the relative phases of the first- and third-order amplitudes. A similar phase produces an enhanced absorption rate (denoted by a common sign for $M_{fi}^{(1)}$ and $M_{fi}^{(3)}$) and dissimilar phases provide a decreased rate (opposite signs). The quantum amplitude for one-photon absorption, $M_{fi}^{(1)}$, is well-known [43], and the one for laser-modified absorption, $M_{fi}^{(3)}$, is given by [52]

$$M_{fi}^{(3)} = ink'k^{\frac{1}{2}} \left(\frac{\hbar c}{2\epsilon_0 V} \right)^{\frac{3}{2}} \bar{e}_i e'_j e'_k \beta_{ijk}^{\alpha 0}(-\omega'; \omega', \omega) \tag{8}$$

Here, the resonant photon energy is $\hbar ck \equiv \hbar\omega$ and e denotes the corresponding polarization vector. When the same symbols carry a prime, they refer to the separately controllable throughput beam. In this formulation, the latter can accommodate arbitrary polarization. Once again, the overbar denotes

complex conjugation (signifying a polarization state that is effectively reflected in the equator of a Poincaré sphere). The quasi-hyperpolarizability $\beta_{ijk}^{\alpha 0}(-\omega'; \omega', \omega)$ has a similar form to Equation (6), but now involves both resonant and non-resonant beams and the real, excited state α . Once again, the order of indices in the tensor correlates with the order of frequency arguments—the explicit form is given in [52]. Through deployment of the explicit expression for $M_{fi}^{(1)}$ and $M_{fi}^{(3)}$, the rate for laser-modified one-photon absorption, Γ_{abs} , emerges as

$$\Gamma_{\text{abs}} = \left(\frac{\pi \rho I}{c \hbar \epsilon_0} \right) e_i \bar{e}_j \left[\mu_i^{(0)\alpha 0} \bar{\mu}_j^{(0)\alpha 0} + (I'/c\epsilon_0) \mu_i^{(0)\alpha 0} \bar{\mu}_j^{(2)\alpha 0}(\omega') + \left(I'^2/4c^2\epsilon_0^2 \right) \mu_i^{(2)\alpha 0}(\omega') \bar{\mu}_j^{(2)\alpha 0}(\omega') \right], \tag{9}$$

in which $I = n\hbar c^2 k/V$ is the irradiance of the absorbing resonant beam and I' is the throughput laser irradiance. It is the second term (linear in I') that signifies a quantum interference of the two amplitudes. This represents the leading correction to the one-photon absorption rate. Equation (9) affords a re-interpretation of earlier expression: One-photon absorption (independent of the off-resonant beam) relates to an effective excitation dipole whose zeroth order is labeled $\mu^{(0)\alpha 0} \equiv \mu^{\alpha 0}$, and the contribution that is quadratic in the electric field (linear in the intensity) of the off-resonant beam is $\mu_i^{(2)\alpha 0}(\omega') \equiv e' j \bar{e}'_k \beta_{ijk}^{\alpha 0}(-\omega'; \omega', \omega)$. The former signifies direct resonant absorption, while the latter a nonlinear amendment comprising the off-resonant radiation of frequency ω' (corresponding to elastic, forward scattering). The off-resonant beam thus effects a modification of the excitation dipole moment via $\mu^{(2)\alpha 0}(\omega')$. The size of the correction term, which can enhance or diminish the spectral intensity of each absorption band, depends on both the intensity of the off-resonant ancillary beam and its fixed frequency. If the fixed frequency lies anywhere in the wings of an absorption band as depicted by Figure 3a,b, from a different (preferably higher) frequency region than the range of the linear absorption measurements, then the associated near-resonance enhancement of the quasi-hyperpolarizability tensor may contribute many further orders of magnitude enhancement to the significance of laser-modified effects.

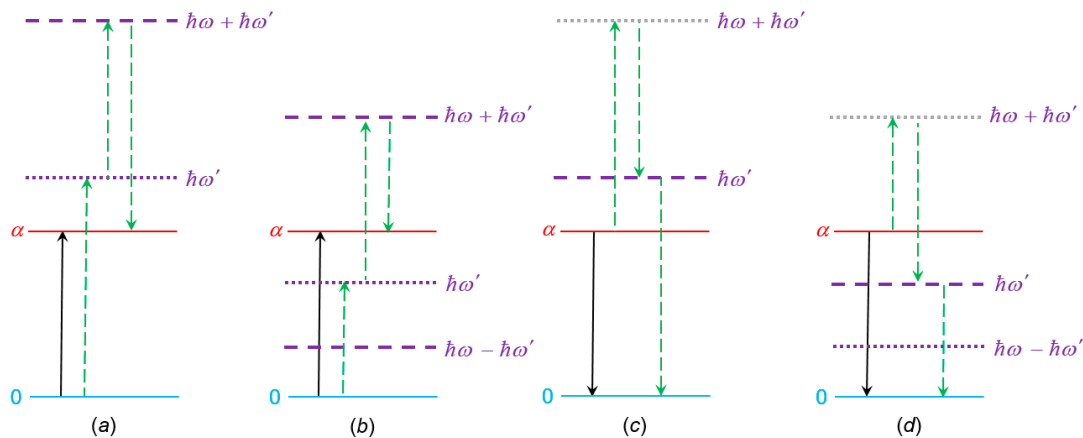


Figure 3. Positions of potential resonance levels for laser-modified single-photon processes of absorption (a,b) and fluorescence (c,d). For simplicity, the off-resonant beam is not shown. In each instance, the vertical black arrow shows the overall transition, and green dotted arrows together denote a sequence for one of the interaction permutations approaching one or more resonances; a purple dotted line indicates a one-photon resonance level and a purple dashed line indicates a two-photon resonance; grey dotted lines indicate an energetically forbidden resonance: (a) single-photon absorption of optical frequency ω , with off-resonant frequency $\omega' > \omega$; (b) as in (a), with $\omega' < \omega$; (c) single-photon emission at frequency ω , with off-resonant frequency $\omega' > \omega$; (d) as in (c), with $\omega' < \omega$.

It is interesting that excitation of a molecule to a metastable state, i.e., one that is one-photon forbidden by orbital symmetry properties, may become possible by input of the off-resonant beam,

since the resulting three-photon mechanism for access to a conventionally symmetry-unfavorable state could then become allowed [55]. This enables a population of a ‘dark’ state—a transition that would otherwise be improbable. For such an effect to occur would, however, demand the levels of intensity routinely associated with three-photon absorption measurements. In another connection with multiphoton absorption, it is also noteworthy that an off-resonant beam can alter the rate of two-photon absorption through a fourth-order perturbation effect [52].

4. Laser-Modified Fluorescence

Following electronic excitation of a molecule—and in the absence of phosphorescence arising from inter-system crossing—there are usually two major relaxation routes: One is fluorescent emission, the subject of this section, and the other is energy transfer to a second ‘acceptor’ molecule (discussed in Section 5). Since, in terms of quantum electrodynamics, light emission is simply time-reversed absorption, the passing of off-resonant laser light of sufficient intensity through an excited molecular system can evidently enhance or suppress the fluorescent emission in an analogous fashion to its effect on absorption. When no light is present, i.e., when the resonant radiation responsible for the initial excitation has left the system, fluorescence once again involves a single photon-molecule interaction that relates to the first term of Equation (4). However, this is not the case when the system is irradiated by the off-resonant beam. Here again, three concerted photon-molecule couplings arise, as shown by Figure 2(b), corresponding to the third term of Equation (4). This contrasts with stimulated emission, which involves the delivery of radiation with a frequency that must match the fluorescence.

The intensity of fluorescence (power per unit solid angle [46]), $I(\Omega)$, is the Fermi emission rate multiplied by the energy of a fluorescent photon, $\hbar ck$, so that the leading contributions are given by [54]

$$I(\Omega) = \left(\frac{ck^4}{8\pi^2\epsilon_0} \right) \bar{e}_i e_j \left[\mu_i^{(0)0\alpha} \bar{\mu}_j^{(0)0\alpha} + (I'/c\epsilon_0) \mu_i^{(0)0\alpha} \bar{\mu}_j^{(2)0\alpha}(\omega') \right. \\ \left. + (I'^2/4c^2\epsilon_0^2) \mu_i^{(2)0\alpha}(\omega') \bar{\mu}_j^{(2)0\alpha}(\omega') \right], \quad (10)$$

which can be interpreted as emission associated with the effective fluorescence-decay (second-order) transition moment $\mu_i^{(2)0\alpha}(\omega') \equiv \bar{e}'_j e'_k \beta_{ijk}^{0\alpha}(\omega; -\omega', \omega')$, where the explicit form of the hyperpolarizability β_{ijk} is similar to that of laser-modified absorption [56]. Again, it is the quantum interference term (the second one, linearly dependent on I') that represents the leading correction to the emission intensity without the throughput beam. The term that is quadratically dependent on I' relates to a special condition that we return to in Section 6. Most often, it will prove negligible compared to the first two terms in Equation (10). Nonetheless, for both terms involving I' , pre-resonance enhancement is again possible: Judicious choice of wavelength for the throughput beam may enhance the magnitude of the second-order transition moment through its dependence on the dispersion properties of the pseudo-hyperpolarizability tensor. This possibility is shown in Figure 3c,d.

A quantity known as the fluorescence anisotropy, r , is an important element in many fluorescence studies. This is determined from the general expression $r = (I_{\parallel} - I_{\perp}) / (I_{\parallel} + 2I_{\perp})$, where I_{\parallel} and I_{\perp} are fluorescence intensities measured through polarizers oriented parallel and perpendicular, respectively, to the polarization of the excitation beam. When the laser-modified interaction comes into play, the effect on the fluorescence anisotropy becomes significantly more intricate, but it may be simplified to an experimentally tractable form based on a two-level approximation. Under such conditions, it has been shown that the following expression for the anisotropy arises [56]

$$r = \frac{3\cos^2\phi - 1 + (KI'/c\epsilon_0)(\cos^2\phi - 1)}{5 + (KI'/7c\epsilon_0)(20 - 11\cos^2\phi)} \quad (11)$$

where ϕ is the angle between the absorption and emission transition moments, the former relating to the resonant laser beam that induces excitation prior to the fluorescence, and the hyperpolarizability

has been simplified to $K|\mu^{0\alpha}|^3$ for calculational convenience (the dipole moments cancel out in r). For the limiting case when $I = 0$, i.e., the off-resonant beam is absent, the well-known expression [57] $r = (1/5)(3\cos^2\phi - 1)$ is recovered.

The modification of individual molecular emission rates is measurable in more than one other respect. An aspect that is principally of spectroscopic interest is the associated change in the decay lifetime, signifying the kinetics of ensemble photophysics. Once again, the capacity to controllably modify this parameter, itself the direct focus in fluorescence lifetime imaging (FLIM) studies for example [58], affords another dimension to resolve differences between chemically distinct fluorophores in close proximity, especially in cases where the corresponding extent of emission spectrum overlap fails to permit speciation by wavelength alone.

It is significant that the input of the off-resonant beam can also alter the near-field spatial distribution of the fluorescent emission [59,60]. Via the nonlinear couplings, the emitted electromagnetic field has an increasingly 'directed' character, i.e., a propagation behavior typically observed in the far-field, as the intensity of the off-resonant beam increases. The phenomenon, therefore, offers the ability to optically control the near-field distribution of fluorescence. Contour maps illustrating the effects of the off-resonant beam on the emission field are provided in Figure 4. It is interesting to note the possibility of using the actively controllable effect we have described either instead of, or in conjunction with, other passive schemes for achieving highly directed output. The virtues of plasmonic enhancement and phased-array nanoantennas for directed emission have recently received prominent interest (see, for example, [61–64]).

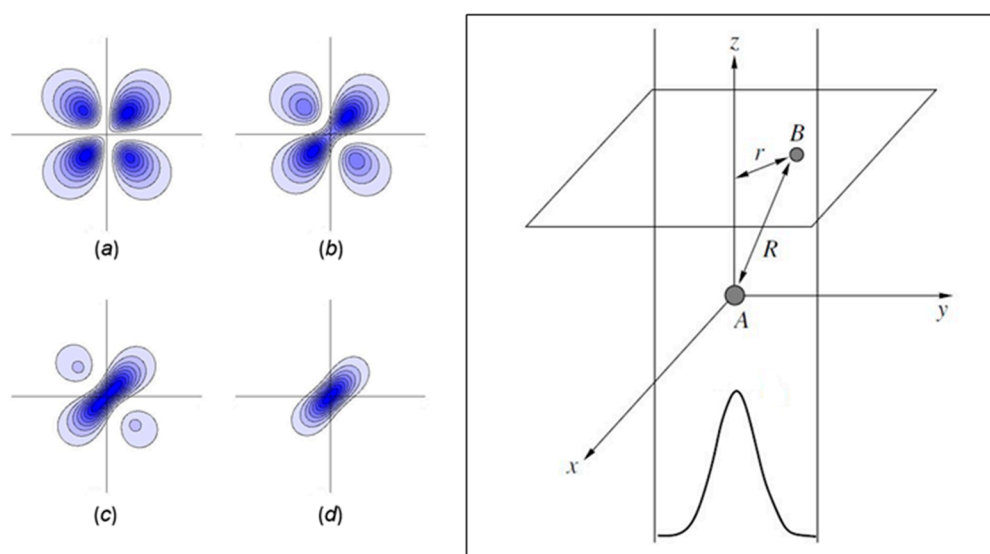


Figure 4. Contour maps of the fluorescence rate, against x and y (both over the range -100 nm, 100 nm) with $z = 40$ nm, from a light-emitting molecule at the source to a detector positioned in the x,y -plane. Here, the input intensity of the off-resonant beam is: (a) 3×10^{11} W cm $^{-2}$, (b) 1×10^{12} W cm $^{-2}$, (c) 2×10^{12} W cm $^{-2}$, and (d) 3×10^{12} W cm $^{-2}$. The darker the shade of blue, the higher the rate. The right-hand diagram shows the model geometry, which involves the source A and detector B at a separation R , while r is the distance of the detector from the z -axis. The input beam, with a Gaussian profile, propagates upward along the z -axis. The beam waist parameter $w = 500$ nm, transition dipole magnitude is 5 D, and both the source and detector bandgap = 0.3 eV. Modified from the original image in [60].

5. Optically Controlled Resonance Energy Transfer

Resonance energy transfer (RET) is the transport of the electronic excitation between electronically distinct molecular components, commonly designated donor A and acceptor B [65–70]. Analogous to the effects of laser-modified absorption and fluorescence, an off-resonant beam of sufficient intensity

is able to increase or reduce the rate of such energy transfer. Again, the key equations are derived in the form of a Fermi rate expression, but this time via $\Gamma_{\text{ret}} \sim \left| M_{fi}^{(2)} + M_{fi}^{(4)} \right|^2$ where $M_{fi}^{(2)}$ and $M_{fi}^{(4)}$ are the quantum amplitudes for the second-order (single-photon emission at A and single-photon absorption at B, i.e., RET) and fourth-order interaction processes (optically controlled RET, also called laser-assisted RET, or LARET), respectively. In detail, optically controlled RET is the process whereby energy transfer proceeds with concurrent absorption of an off-resonant beam at A and re-emission at B (and vice-versa). RET intrinsically involves the emission and annihilation of a virtual photon [71]. Thus, four photon-molecule interactions are involved overall, as shown in Figure 2c, and the precise form of the associated quantum amplitude is accordingly secured from the fourth term in Equation (4). In the near field, where RET is most commonly measured, the quantum amplitude of the laser-modified process is given by [72,73]

$$M_{fi}^{(4)} = \left(\frac{I'}{2\epsilon_0 c} \right) e_i \bar{e}_l V_{jk}(0, \mathbf{R}) \left(\alpha_{ij}^{0\alpha(A)}(-\omega') \alpha_{lk}^{0\beta(B)}(\omega') + \alpha_{ij}^{0\beta(B)}(-\omega') \alpha_{lk}^{0\alpha(A)}(\omega') \right) \quad (12)$$

where $-\alpha_{ij}$ is a transition polarizability, β is an excited state of B (for simplicity, denoted α in Figure 2c) and $V_{jk}(0, \mathbf{R})$ is the dipole-dipole coupling tensor, which acquires the form of its static limit in the near-field. The rate of optically controlled resonance energy transfer is found from Equation (12) and the matrix element, $M_{fi}^{(2)}$, for conventional RET [43], to give

$$\Gamma_{\text{ret}} = V_{jk}(0, \mathbf{R}) V_{mn}(0, \mathbf{R}) \left[\mu_j^{0\alpha(A)} \mu_k^{0\beta(B)} \mu_m^{0\alpha(A)} \mu_n^{0\beta(B)} + (I'/c\epsilon_0) e_i \bar{e}_l \mu_m^{0\alpha(A)} \mu_n^{0\beta(B)} \times \left(\alpha_{ij}^{0\alpha(A)}(-\omega') \alpha_{lk}^{0\beta(B)}(\omega') + \alpha_{ij}^{0\beta(B)}(-\omega') \alpha_{lk}^{0\alpha(A)}(\omega') \right) + \dots \right] \quad (13)$$

Here, the first term is the rate of RET as it occurs without the input beam, and the second term is the quantum interference between RET and optically controlled RET. The latter term, linear in the irradiance of the off-resonant laser beam, is the leading correction to the transfer rate when the laser beam is present.

One of the ancillary benefits of using a QED framework to elicit theory is that its uniform systematization of interactions often enables the recognition and identification of connections between what might otherwise be considered entirely unrelated effects. Here, for example, it emerged that optically controlled resonance energy transfer is closely related in its fundamental mechanism to the well-known optomechanical phenomenon known as optical binding [74–85]. The latter process again involves an off-resonant laser beam that can increase (or decrease) an existing effect. In the case of molecules, it produces a laser-induced optical force at levels that can extend significantly beyond that of the Casimir–Polder force [86–90] (whose effects pervade any system of neutral molecules). Since, in the case of optical binding, the initial and final molecular states are identical ground states, i.e., the excited states α and β do not arise, a force is determined rather than a rate [91]. However, in terms of quantum electrodynamics, the mathematics and the mechanisms are similar. Our very recent review on the latest research on optical binding at the nanoscale can be found elsewhere [92].

6. All-Optical Switching

The possibility of all-optical switching—in which light is controlled by light—is apparent when a forbidden optical process becomes allowed when subjected to an off-resonant optical input. At the molecular level, this will usually be either one-photon absorption, fluorescence, or resonance energy transfer. For example, a potential set-up (discussed below) based on the latter is shown in Figure 5. All these prospects provide a basis for an all-optical switch since the throughput and absence of the off-resonant signal results in the activation and deactivation of the optical process, respectively. All-optical switching based on dipole transition properties has the distinct advantage of ultrafast operation, compared to most electronic or even optomechanical mechanisms. Moreover, in the ultrafast

regime, it is possible to entertain switching that is sustained throughout the duration of an input pulse, rather than requiring the activating input to act as a trigger for a state that will persist beyond the input.

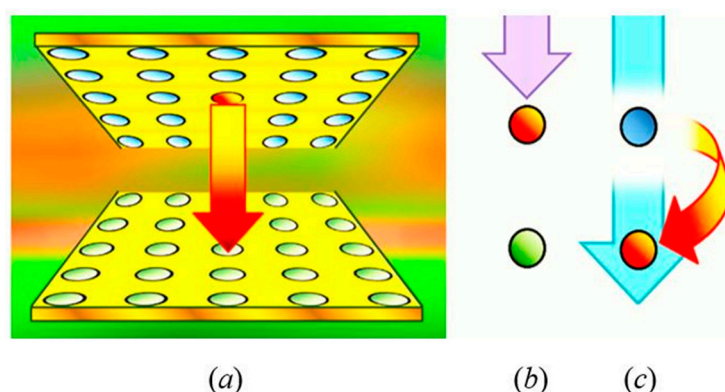


Figure 5. Depiction of optically controlled resonance energy transfer (RET). (a) Energy transfer from an excited donor in the upper array of quantum dots to its partner below (spacer material not shown). The transition dipoles lie in the respective planes and are mutually perpendicular. (b) Before off-resonant beam enters the system, no energy transfer occurs from the excited quantum dot (red circle) to its partner (green circle). (c) On input of the off-resonant beam, energy is transferred from the donor (blue circle) to the acceptor.

When an optical process without the input beam is forbidden, either by the polarization geometry, or by virtue of selection rules, it is notable that both the first and second (interference) terms in Equations (9), (10), and (13) are null. In each case, only the final nonlinear term remains. As discussed earlier, molecules of relatively high symmetry may frequently possess electronic excited states that are accessible by three-quantum, but not single-quantum, transitions. Notably, the selection rules for an electric octupole transition still subsume those for a simple electric dipole [93]. However, in systems where each component of the sample has a common, fixed, orientation—as, for example, in a nematic liquid crystal—then it is possible to arrange experimental conditions such that any specific, single-photon allowed process will be precluded using linearly polarized resonant input whose polarization vector is orthogonal to the conventional transition dipole. Then, the same transition may be allowed through non-zero, off-diagonal components of the transition quasi-hyperpolarizability. This represents a straightforward geometric configuration for effectively switching on or off the associated transition, a simple instance of all-optical switching.

Resonance energy transfer can also be prohibited either by a suitable geometric configuration, in which the transition dipole moments of the donor and acceptor and the displacement vector are mutually orthogonal, or by a one-photon symmetry-forbidden electronic transition in the donor or acceptor. To develop an all-optical switch model, using the concepts of the last section, the case of a pair of parallel two-dimensional square-lattice arrays has been studied—with one a donor array and the other an acceptor array, each comprising a set of equally spaced, identical, and optically distinct antennas. The donor species are chemically dissimilar from the acceptors to preclude back-transfer [94], and the two arrays were constructed so that each constituent of the donor array corresponds to a component within the acceptor array. The effective capacity for energy transfer from an emitter in the donor array (assumed at the origin) to be directed to its designated partner in the acceptor array can be quantified by comparing it to the summed efficiencies for transfer to all other molecules within either array, i.e., the cross talk. Presuming typical values for the variables, the aspect ratio (where r is the distance between the arrays and l is the lattice constant) can be 0.3 for $I' = 1 \times 10^{12} \text{ W cm}^{-2}$ or 0.06 for $1 \times 10^{10} \text{ W cm}^{-2}$ to achieve transfer losses less than 5%. This demonstrates that the irradiance of the off-resonant beam is a major contributing factor in the destination of the donor excitation [53].

The next goal would be the optical control of a 2D-distributed binary coding—where 1 and 0 denote excited and unexcited molecules, respectively—by manipulating the excitation transfer

from multiple molecules in the donor (input) array to their partners in the acceptor (output) array. In other words, the binary pattern on the donor array is controllably transferred to the acceptor array, signifying parallel processing capability [95]. The output array is then ‘read’ by detection of the emission that follows the relaxation of the acceptors. Another all-optical binary system is conceivable via a combination of laser-modified absorption and fluorescence. When conventional absorption and fluorescence cannot undergo linear engagement, i.e., transitions to the electronic excited state are one-photon forbidden by symmetry, nonlinear activation of the process may be possible on input of the off-resonant beam. This all-optical switching principle could lead to the intriguing possibility that binary data is controllably written, through laser-modified absorption, to a molecule with a metastable state and read using the analogous laser-modified emission technique. Such a device will again be confined to the realm of ultrafast processing, in which a temporary data register of a few nanoseconds is sufficiently long-lived. It is noteworthy that the contour maps of Figure 4 also show all-optical switching in that, if the probe is positioned on the z -axis, no emission is detected when the off-resonant beam is off, but emission is activated at any interval when the beam is switched on.

Another feasible scheme is an optical transistor, based on the principle that the off-resonant beam can optically control the amount of stimulated emission from a three-level lasing material pumped just below its threshold. A model analysis demonstrates that an input beam of sufficient intensity modifies the amplification kinetics of the active medium and thereby enhances laser output [96]. For a constant pumping rate, at a level indicated by the dotted vertical line (see Figure 6), the system operates below threshold when the input beam is absent. On introduction of the beam with an irradiance approaching $2 \times 10^{11} \text{ W cm}^{-2}$, output may climb by approximately 14 orders of magnitude, rising to 16 orders if the input intensity is doubled—a phase transition feature that is typical of a laser operating at and above threshold. The beauty of this scheme is that its operation is not limited to any specific material. To summarize, the feasibility of conferring optical nonlinearity upon photoactive materials leads to mechanistic features with a range of potential applications, such as all-optical switching and transistor action.

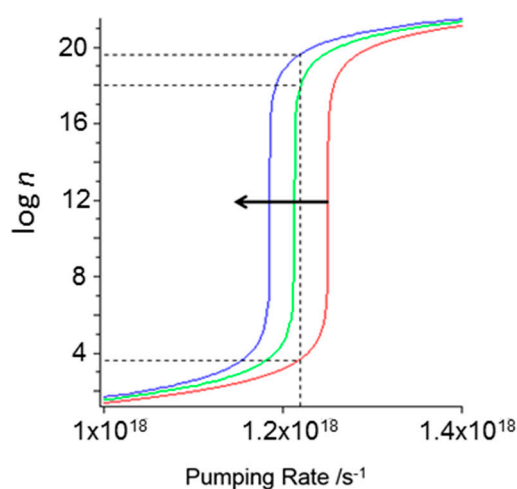


Figure 6. The number of emitted photons, plotted as $\log n$, against the pumping rate in the absence (red line) and presence of an off-resonant beam. The irradiance of the probe beam is $2 \times 10^{11} \text{ W cm}^{-2}$ (green) and $4 \times 10^{11} \text{ W cm}^{-2}$ (blue). The lasing threshold, as indicated by the sudden increase in n , reduces with increasing intensity of the probe beam. With suitable pumping, a shift to above-threshold operation is observed (upper dotted lines). Modified from the original image in [96].

7. Discussion

The primary discoveries associated with the off-resonant modification of optical processes were entertained in connection with their potential deployment in spectroscopic and photophysical measurements. At the simplest level, additional control is afforded by the capacity to vary the intensity,

polarization, wavelength, and even pulse duration of the off-resonant beam, representing an expanded parameter space for experimentation. Although it has yet to receive detailed analysis, it is not only the intensity of individual bands in a spectrum that may exhibit change under suitable conditions: A modification to line-shapes may also be anticipated.

The possibility of achieving all-optical switching now represents one of the more recently attractive propositions for application. Although the speed of ultrafast communications and computer processing continues unabated, they have until now still been essentially subject to Moore's Law. For many years, it has been known that the long-sought goal of all-optical switching has the capacity to revolutionize telecommunications and computing, since the relatively slow and energetically inefficient opto-electronic conversions that form bottlenecks in present technology can be circumvented. Therefore, unsurprisingly, numerous implementation strategies have been proposed, some of which are now briefly discussed.

One technique involves the optical control of the refractive index of a material, so that a secondary beam travelling through the medium can be modified in speedily reversible manner [97]. Closely related are systems that exploit electromagnetic induced transparency [98–100], in which a material becomes transparent within a narrow range of the absorption spectrum. Similar all-optical switching arrangements are based on Mach–Zehnder interferometry [101,102]. Other schemes make use of semiconductor nanoparticles [103–105], nanoplasmonic waveguides [106–109], fiber Bragg gratings [110–112] or nanocavities in photonic crystals to strongly enhance optical nonlinearities [113,114]. Moreover, based on irradiation of rubidium vapor, there is a development that uses counter-propagating laser beams to induce an optical pattern that rotates on application of a switching laser [115]. Compared to the approach we describe, many of these methods suffer the disadvantage of requiring optical structures and configurations substantially larger than typical molecular dimensions. Moreover, although there are indeed other specifically molecule-based methods, such as several based on the photocycle of bacteriorhodopsin [116,117], their speed is significantly constrained by the kinetics of state interconversion, each with a finite (typically picosecond) lifetime. The progress of these and many other all-optical systems have been discussed in two excellent reviews [118,119]. It is still clear, at present, that no single scheme has been adopted as the one that will be useful in a practicable device in the near future.

The prospect we have identified of controlling resonance energy transfer without requiring a microcavity [120] is most likely to involve all-optical switching implemented in a synthetic heterostructure. Building such a device requires exploitation of the recent advances in the construction of quantum dot arrays—see, for example, [121,122]—here, with juxtaposed arrays sandwiching an optically transparent spacer layer. Technical realizations are expected to implement the most suitable nanofabrication method, such as dip-pen nanolithography. The advantage of such a system is its viable operation at short ultraviolet/visible wavelengths without the use of expensive, non-standard optical elements. Above all, it offers a high-information density and ultrafast response with high repetition rate and high efficiency. The initial work on optical transistor action, based on the optical control of fluorescence, may also break ground for the broader development of novel all-optical methods. Such opportunities are not limited to device applications. They offer clear advantages over molecular switches since their operation does not require atomic motion, and the switching times are much faster since they are comparable to excited state decay. It is hoped that, with the ongoing progress of optoelectronics, a new generation of optical devices tailored for telecommunications and IT will emerge in the near future.

Author Contributions: The contributions of each author to this Review—including writing, equation and figure production, reviewing, drafting and proof-reading – is: D.S.B. 40%, D.L.A. 35% and K.A.F. 25%. The original research was by D.S.B. and D.L.A.

Funding: K.A.F. is funded by the Leverhulme Trust under the Grant Number ECF-2019-398.

Acknowledgments: K.A.F. would like to thank the Leverhulme Trust for funding through a Leverhulme Early Career Fellowship.

Conflicts of Interest: The authors declare no conflict of interest.

References

1. Bloembergen, N. *Nonlinear Optics*, 4th ed.; World Scientific: Singapore, 1996.
2. Jha, S.S. *Perspectives in Optoelectronics*; World Scientific: Singapore, 1995.
3. Sauter, E.G. *Nonlinear Optics*; Wiley: New York, NY, USA, 1996.
4. He, G.; Liu, S.H. *Physics of Nonlinear Optics*; World Scientific: Singapore, 2000.
5. Shen, Y.R. *The Principles of Nonlinear Optics*; Wiley: New York, NY, USA, 2002.
6. Sutherland, R.L. *Handbook of Nonlinear Optics*, 2nd ed.; Dekker: New York, NY, USA, 2003.
7. Banerjee, P.P. *Nonlinear Optics: Theory, Numerical Modeling, and Applications*; Dekker: New York, NY, USA, 2003.
8. Novotny, L.; Hecht, B. *Principles of Nano-Optics*; Cambridge University Press: Cambridge, UK, 2006.
9. Boyd, R.W. *Nonlinear Optics*, 3rd ed.; Academic Press: New York, NY, USA, 2008.
10. Lvovsky, A.I.; Mlynek, J. Quantum-optical catalysis: Generating nonclassical states of light by means of linear optics. *Phys. Rev. Lett.* **2002**, *88*, 250401. [[CrossRef](#)] [[PubMed](#)]
11. Hu, L.-Y.; Wu, J.-N.; Liao, Z.; Zubairy, M.S. Multiphoton catalysis with coherent state input: Nonclassicality and decoherence. *J. Phys. B At. Mol. Opt. Phys.* **2016**, *49*, 175504. [[CrossRef](#)]
12. Hu, L.; Liao, Z.; Zubairy, M.S. Continuous-variable entanglement via multiphoton catalysis. *Phys. Rev. A* **2017**, *95*, 012310. [[CrossRef](#)]
13. Zhou, W.; Ye, W.; Liu, C.; Hu, L.; Liu, S. Entanglement improvement of entangled coherent state via multiphoton catalysis. *Laser Phys. Lett.* **2018**, *15*, 065203. [[CrossRef](#)]
14. Ye, W.; Zhong, H.; Liao, Q.; Huang, D.; Hu, L.; Guo, Y. Improvement of self-referenced continuous-variable quantum key distribution with quantum photon catalysis. *Opt. Express* **2019**, *27*, 17186–17198. [[CrossRef](#)] [[PubMed](#)]
15. Hilsabeck, K.I.; Meiser, J.L.; Sneha, M.; Harrison, J.A.; Zare, R.N. Nonresonant photons catalyze photodissociation of phenol. *J. Am. Chem. Soc.* **2019**, *141*, 1067–1073. [[CrossRef](#)] [[PubMed](#)]
16. Cushing, S.K.; Li, J.; Meng, F.; Senty, T.R.; Suri, S.; Zhi, M.; Li, M.; Bristow, A.D.; Wu, N. Photocatalytic activity enhanced by plasmonic resonant energy transfer from metal to semiconductor. *J. Am. Chem. Soc.* **2012**, *134*, 15033–15041. [[CrossRef](#)] [[PubMed](#)]
17. Gonzaga-Galeana, J.A.; Zurita-Sánchez, J.R. A revisit of the Förster energy transfer near a metallic spherical nanoparticle: (1) Efficiency enhancement or reduction? (2) The control of the Förster radius of the unbounded medium. (3) The impact of the local density of states. *J. Chem. Phys.* **2013**, *139*, 244302. [[CrossRef](#)] [[PubMed](#)]
18. Schleifenbaum, F.; Kern, A.M.; Konrad, A.; Meixner, A.J. Dynamic control of Förster energy transfer in a photonic environment. *Phys. Chem. Chem. Phys.* **2014**, *16*, 12812–12817. [[CrossRef](#)]
19. Li, J.; Cushing, S.K.; Meng, F.; Senty, T.R.; Bristow, A.D.; Wu, N. Plasmon-induced resonance energy transfer for solar energy conversion. *Nat. Photonics* **2015**, *9*, 601. [[CrossRef](#)]
20. Ghenuche, P.; Mivelle, M.; de Torres, J.; Moparthi, S.B.; Rigneault, H.; Van Hulst, N.F.; García-Parajó, M.F.; Wenger, J. Matching nanoantenna field confinement to FRET distances enhances Förster energy transfer rates. *Nano Lett.* **2015**, *15*, 6193–6201. [[CrossRef](#)] [[PubMed](#)]
21. Konrad, A.; Metzger, M.; Kern, A.M.; Brecht, M.; Meixner, A.J. Controlling the dynamics of Förster resonance energy transfer inside a tunable sub-wavelength Fabry–Pérot-resonator. *Nanoscale* **2015**, *7*, 10204–10209. [[CrossRef](#)] [[PubMed](#)]
22. Tumkur, T.U.; Kitur, J.K.; Bonner, C.E.; Poddubny, A.N.; Narimanov, E.E.; Noginov, M.A. Control of Förster energy transfer in the vicinity of metallic surfaces and hyperbolic metamaterials. *Faraday Discuss.* **2015**, *178*, 395–412. [[CrossRef](#)] [[PubMed](#)]
23. Bidault, S.; Devilez, A.; Ghenuche, P.; Stout, B.; Bonod, N.; Wenger, J. Competition between Förster resonance energy transfer and donor photodynamics in plasmonic dimer nanoantennas. *ACS Photonics* **2016**, *3*, 895–903. [[CrossRef](#)]
24. de Torres, J.; Ferrand, P.; Colas des Francs, G.; Wenger, J. Coupling emitters and silver nanowires to achieve long-range plasmon-mediated fluorescence energy transfer. *ACS Nano* **2016**, *10*, 3968–3976. [[CrossRef](#)]

25. Poudel, A.; Chen, X.; Ratner, M.A. Enhancement of resonant energy transfer due to an evanescent wave from the metal. *J. Phys. Chem. Lett.* **2016**, *7*, 955–960. [[CrossRef](#)]
26. Marocico, C.A.; Zhang, X.; Bradley, A.L. A theoretical investigation of the influence of gold nanosphere size on the decay and energy transfer rates and efficiencies of quantum emitters. *J. Chem. Phys.* **2016**, *144*, 024108. [[CrossRef](#)]
27. Wubs, M.; Vos, W.L. Förster resonance energy transfer rate in any dielectric nanophotonic medium with weak dispersion. *New J. Phys.* **2016**, *18*, 053037. [[CrossRef](#)]
28. Higgins, L.J.; Marocico, C.A.; Karanikolas, V.D.; Bell, A.P.; Gough, J.J.; Murphy, G.P.; Parbrook, P.J.; Bradley, A.L. Influence of plasmonic array geometry on energy transfer from a quantum well to a quantum dot layer. *Nanoscale* **2016**, *8*, 18170–18179. [[CrossRef](#)]
29. Bujak, Ł.; Ishii, T.; Sharma, D.K.; Hirata, S.; Vacha, M. Selective turn-on and modulation of resonant energy transfer in single plasmonic hybrid nanostructures. *Nanoscale* **2017**, *9*, 1511–1519. [[CrossRef](#)]
30. Murphy, G.P.; Gough, J.J.; Higgins, L.J.; Karanikolas, V.D.; Wilson, K.M.; Garcia Coindreau, J.A.; Zubialeovich, V.Z.; Parbrook, P.J.; Bradley, A.L. Ag colloids and arrays for plasmonic non-radiative energy transfer from quantum dots to a quantum well. *Nanotechnology* **2017**, *28*, 115401. [[CrossRef](#)] [[PubMed](#)]
31. Steele, J.M.; Ramnarace, C.M.; Farner, W.R. Controlling FRET enhancement using plasmon modes on gold nanogratings. *J. Phys. Chem. C* **2017**, *121*, 22353–22360. [[CrossRef](#)]
32. Akulov, K.; Bochman, D.; Golombek, A.; Schwartz, T. Long-distance resonant energy transfer mediated by hybrid plasmonic-photonic modes. *J. Phys. Chem. C* **2018**, *122*, 15853–15860. [[CrossRef](#)]
33. Asgar, H.; Jacob, L.; Hoang, T.B. Fast spontaneous emission and high Förster resonance energy transfer rate in hybrid organic/inorganic plasmonic nanostructures. *J. Appl. Phys.* **2018**, *124*, 103105. [[CrossRef](#)]
34. Eldabagh, N.; Micek, M.; DePrince, A.E.; Foley, J.J. Resonance energy transfer mediated by metal-dielectric composite nanostructures. *J. Phys. Chem. C* **2018**, *122*, 18256–18265. [[CrossRef](#)]
35. Glaeske, M.; Juergensen, S.; Gabrielli, L.; Menna, E.; Mancin, F.; Gatti, T.; Setaro, A. PhysicaPlasmon-assisted energy transfer in hybrid nanosystems. *Phys. Status Solidi Rapid Res. Lett.* **2018**, *12*, 1800508. [[CrossRef](#)]
36. Roth, D.J.; Nasir, M.E.; Ginzburg, P.; Wang, P.; Le Marois, A.; Suhling, K.; Richards, D.; Zayats, A.V. Förster resonance energy transfer inside hyperbolic metamaterials. *ACS Photonics* **2018**, *5*, 4594–4603. [[CrossRef](#)]
37. Wu, J.-S.; Lin, Y.-C.; Sheu, Y.-L.; Hsu, L.-Y. Characteristic distance of resonance energy transfer coupled with surface plasmon polaritons. *J. Phys. Chem. Lett.* **2018**, *9*, 7032–7039. [[CrossRef](#)]
38. Zurita-Sánchez, J.R.; Méndez-Villanueva, J. Förster energy transfer in the vicinity of two metallic nanospheres (dimer). *Plasmonics* **2018**, *13*, 873–883. [[CrossRef](#)]
39. Olivo, J.; Zapata-Rodríguez, C.J.; Cuevas, M. Spatial modulation of the electromagnetic energy transfer by excitation of graphene waveguide surface plasmons. *J. Opt.* **2019**, *21*, 045002. [[CrossRef](#)]
40. Bohlen, J.; Cuartero-González, Á.; Pibiri, E.; Ruhlandt, D.; Fernández-Domínguez, A.I.; Tinnefeld, P.; Acuna, G.P. Plasmon-assisted Förster resonance energy transfer at the single-molecule level in the moderate quenching regime. *Nanoscale* **2019**, *11*, 7674–7681. [[CrossRef](#)] [[PubMed](#)]
41. Wang, Y.; Li, H.; Zhu, W.; He, F.; Huang, Y.; Chong, R.; Kou, D.; Zhang, W.; Meng, X.; Fang, X. Plasmon-mediated nonradiative energy transfer from a conjugated polymer to a plane of graphene-nanodot-supported silver nanoparticles: An insight into characteristic distance. *Nanoscale* **2019**, *11*, 6737–6746. [[CrossRef](#)] [[PubMed](#)]
42. Wang, Z.; Glesk, I.; Chen, L.R. An integrated nonlinear optical loop mirror in silicon photonics for all-optical signal processing. *APL Photon.* **2018**, *3*, 026102. [[CrossRef](#)]
43. Craig, D.P.; Thirunamachandran, T. *Molecular Quantum Electrodynamics: An Introduction to Radiation-Molecule Interactions*; Dover Publications: Mineola, NY, USA, 1998.
44. Salam, A. *Molecular Quantum Electrodynamics. Long-Range Intermolecular Interactions*; Wiley: Hoboken, NJ, USA, 2010.
45. Grynberg, G.; Aspect, A.; Fabre, C. *Introduction to Quantum Optics: From the Semi-Classical Approach to Quantized Light*; Cambridge University Press: Cambridge, UK, 2010.
46. Andrews, D.L.; Allcock, P. *Optical Harmonics in Molecular Systems*; Wiley-VCH: Weinheim, Germany, 2002.
47. Andrews, D.L.; Bradshaw, D.S. *Introduction to Photon Science and Technology*; SPIE Press: Bellingham, WA, USA, 2018.
48. Andrews, D.L.; Jones, G.A.; Salam, A.; Woolley, R.G. Quantum Hamiltonians for optical interactions. *J. Chem. Phys.* **2018**, *148*, 040901. [[CrossRef](#)] [[PubMed](#)]

49. Atkins, P.W.; Friedman, R.S. *Molecular Quantum Mechanics*; Oxford University Press: Oxford, 2011.
50. Andrews, D.L.; Bradshaw, D.S.; Forbes, K.A.; Salam, A. A guide to quantum and semiclassical electrodynamics in modern optics. *J. Opt. Soc. Am. B* submitted 2019.
51. Hollas, J.M. *Modern Spectroscopy*; Wiley: Chichester, UK, 2004.
52. Bradshaw, D.S.; Andrews, D.L. Laser-modified one- and two-photon absorption: Expanding the scope of optical nonlinearity. *Phys. Rev. A* **2013**, *88*, 033807. [[CrossRef](#)]
53. Bradshaw, D.S.; Andrews, D.L. Optically controlled resonance energy transfer: Mechanism and configuration for all-optical switching. *J. Chem. Phys.* **2008**, *128*, 144506. [[CrossRef](#)]
54. Bradshaw, D.S.; Andrews, D.L. All-optical control of molecular fluorescence. *Phys. Rev. A* **2010**, *81*, 013424. [[CrossRef](#)]
55. Andrews, D.L.; Bradshaw, D.S. Optically tailored access to metastable electronic states. *Chem. Phys. Lett.* **2013**, *590*, 235–238. [[CrossRef](#)]
56. Bradshaw, D.S.; Andrews, D.L. Mechanism for optical enhancement and suppression of fluorescence. *J. Phys. Chem. A* **2009**, *113*, 6537–6539. [[CrossRef](#)]
57. Lakowicz, J.R. *Principles of Fluorescence Spectroscopy*, 2nd ed.; Kluwer Academic: New York, NY, USA, 1999.
58. Valeur, B.; Berberan-Santos, M.N. *Molecular Fluorescence: Principles and Applications*, 2nd ed.; Wiley-VCH: Weinheim, Germany, 2013.
59. Bradshaw, D.S.; Andrews, D.L. The control of near-field optics: Imposing direction through coupling with off-resonant laser light. *Appl. Phys. B* **2008**, *93*, 13–20. [[CrossRef](#)]
60. Bradshaw, D.S.; Andrews, D.L. Laser conferral of a directed character to near-field energy transfer. *Laser Phys.* **2009**, *19*, 125–128. [[CrossRef](#)]
61. Curto, A.G.; Volpe, G.; Taminiau, T.H.; Kreuzer, M.P.; Quidant, R.; van Hulst, N.F. Unidirectional emission of a quantum dot coupled to a nanoantenna. *Science* **2010**, *329*, 930–933. [[CrossRef](#)] [[PubMed](#)]
62. Lin, J.; Mueller, J.P.B.; Wang, Q.; Yuan, G.; Antoniou, N.; Yuan, X.-C.; Capasso, F. Polarization-controlled tunable directional coupling of surface plasmon polaritons. *Science* **2013**, *340*, 331–334. [[CrossRef](#)] [[PubMed](#)]
63. Laux, F.; Bonod, N.; Gérard, D. Single emitter fluorescence enhancement with surface lattice resonances. *J. Phys. Chem. C* **2017**, *121*, 13280–13289. [[CrossRef](#)]
64. Sun, Y.-Z.; Feng, L.-S.; Bachelot, R.; Blaize, S.; Ding, W. Full control of far-field radiation via photonic integrated circuits decorated with plasmonic nanoantennas. *Opt. Express* **2017**, *25*, 17417–17430. [[CrossRef](#)] [[PubMed](#)]
65. van der Meer, B.W.; Coker, G.; Chen, S.Y.S. *Resonance Energy Transfer: Theory and Data*; VCH: New York, NY, USA, 1994.
66. Andrews, D.L.; Demidov, A.A. *Resonance Energy Transfer*; Wiley: Chichester, UK, 1999.
67. May, V. *Charge and Energy Transfer Dynamics in Molecular Systems*; John Wiley & Sons: Hoboken, NJ, USA, 2008.
68. Medintz, I.; Hildebrandt, N. *Förster Resonance Energy Transfer: From Theory to Applications*; Wiley-VCH: Weinheim, Germany, 2013.
69. Salam, A. The unified theory of resonance energy transfer according to molecular quantum electrodynamics. *Atoms* **2018**, *6*, 56. [[CrossRef](#)]
70. Jones, G.A.; Bradshaw, D.S. Resonance energy transfer: From fundamental theory to recent applications. *Front. Phys.* **2019**, *7*, 100. [[CrossRef](#)]
71. Andrews, D.L.; Bradshaw, D.S. The role of virtual photons in nanoscale photonics. *Ann. Phys.* **2014**, *526*, 173–186. [[CrossRef](#)]
72. Allcock, P.; Jenkins, R.D.; Andrews, D.L. Laser assisted resonance energy transfer. *Chem. Phys. Lett.* **1999**, *301*, 228–234. [[CrossRef](#)]
73. Allcock, P.; Jenkins, R.D.; Andrews, D.L. Laser-assisted resonance-energy transfer. *Phys. Rev. A* **2000**, *61*, 023812. [[CrossRef](#)]
74. Thirunamachandran, T. Intermolecular interactions in the presence of an intense radiation field. *Mol. Phys.* **1980**, *40*, 393–399. [[CrossRef](#)]
75. Burns, M.M.; Fournier, J.-M.; Golovchenko, J.A. Optical binding. *Phys. Rev. Lett.* **1989**, *63*, 1233–1236. [[CrossRef](#)] [[PubMed](#)]
76. Burns, M.M.; Fournier, J.-M.; Golovchenko, J.A. Optical matter: Crystallization and binding in intense optical fields. *Science* **1990**, *249*, 749–754. [[CrossRef](#)] [[PubMed](#)]

77. Milonni, P.W.; Shih, M.L. Source theory of the Casimir force. *Phys. Rev. A* **1992**, *45*, 4241–4253. [[CrossRef](#)]
78. Dapasse, F.; Vigoureux, J.M. Optical binding force between two Rayleigh particles. *J. Phys. D Appl. Phys.* **1994**, *27*, 914–919. [[CrossRef](#)]
79. Milonni, P.W.; Smith, A. van der Waals dispersion forces in electromagnetic fields. *Phys. Rev. A* **1996**, *53*, 3484–3489. [[CrossRef](#)]
80. Chaumet, P.C.; Nieto-Vesperinas, M. Optical binding of particles with or without the presence of a flat dielectric surface. *Phys. Rev. B* **2001**, *64*, 035422. [[CrossRef](#)]
81. Nieto-Vesperinas, M.; Chaumet, P.C.; Rahmani, A. Near-field photonic forces. *Philos. Trans. R. Soc. A* **2004**, *362*, 719–737. [[CrossRef](#)]
82. Mohanty, S.K.; Andrews, J.T.; Gupta, P.K. Optical binding between dielectric particles. *Opt. Express* **2004**, *12*, 2746–2753. [[CrossRef](#)]
83. Bradshaw, D.S.; Andrews, D.L. Optically induced forces and torques: Interactions between nanoparticles in a laser beam. *Phys. Rev. A* **2005**, *72*, 033816. [[CrossRef](#)]
84. Dholakia, K.; Zemanek, P. Grippled by light: Optical binding. *Rev. Mod. Phys.* **2010**, *82*, 1767–1791. [[CrossRef](#)]
85. Bowman, R.W.; Padgett, M.J. Optical trapping and binding. *Rep. Prog. Phys.* **2013**, *76*, 026401. [[CrossRef](#)] [[PubMed](#)]
86. Casimir, H.B.G.; Polder, D. The influence of retardation on the London-van der Waals forces. *Phys. Rev.* **1948**, *73*, 360–372. [[CrossRef](#)]
87. Buhmann, S.Y.; Knöll, L.; Welsch, D.-G.; Dung, H.T. Casimir-Polder forces: A nonperturbative approach. *Phys. Rev. A* **2004**, *70*, 052117. [[CrossRef](#)]
88. Przybytek, M.; Jeziorski, B.; Cencek, W.; Komasa, J.; Mehl, J.B.; Szalewicz, K. Onset of Casimir-Polder retardation in a long-range molecular quantum state. *Phys. Rev. Lett.* **2012**, *108*, 183201. [[CrossRef](#)] [[PubMed](#)]
89. Salam, A. *Non-Relativistic QED Theory of the van der Waals Dispersion Interaction*; Springer: Cham, Switzerland, 2016.
90. Passante, R. Dispersion interactions between neutral atoms and the quantum electrodynamical vacuum. *Symmetry* **2018**, *10*, 735. [[CrossRef](#)]
91. Bradshaw, D.S.; Andrews, D.L. Interparticle interactions: Energy potentials, energy transfer, and nanoscale mechanical motion in response to optical radiation. *J. Phys. Chem. A* **2013**, *117*, 75–82. [[CrossRef](#)]
92. Forbes, K.A.; Bradshaw, D.S.; Andrews, D.L. Off-resonance nanophotonics: From optical binding and induced self-assembly to all-optical switching. *Nanophoton* **2019**. submitted.
93. Scholes, G.D.; Andrews, D.L. Damping and higher multipole effects in the quantum electrodynamical model for electronic energy transfer in the condensed phase. *J. Chem. Phys.* **1997**, *107*, 5374–5384. [[CrossRef](#)]
94. Andrews, D.L.; Rodríguez, J. Resonance energy transfer: Spectral overlap, efficiency, and direction. *J. Chem. Phys.* **2007**, *127*, 084509. [[CrossRef](#)]
95. Bradshaw, D.S.; Andrews, D.L. All-optical switching between quantum dot nanoarrays. *Superlatt. Microstruct.* **2010**, *47*, 308–313. [[CrossRef](#)]
96. Andrews, D.L.; Bradshaw, D.S. Off-resonant activation of optical emission. *Opt. Commun.* **2010**, *283*, 4365–4367. [[CrossRef](#)]
97. Taghinejad, M.; Cai, W. All-optical control of light in micro- and nanophotonics. *ACS Photonics* **2019**, *6*, 1082–1093. [[CrossRef](#)]
98. Bajcsy, M.; Hofferberth, S.; Balic, V.; Peyronel, T.; Hafezi, M.; Zibrov, A.S.; Vuletic, V.; Lukin, M.D. Efficient all-optical switching using slow light within a hollow fiber. *Phys. Rev. Lett.* **2009**, *102*, 203902. [[CrossRef](#)] [[PubMed](#)]
99. Lee, M.-J.; Chen, Y.-H.; Wang, I.C.; Yu, I.A. EIT-based all-optical switching and cross-phase modulation under the influence of four-wave mixing. *Opt. Express* **2012**, *20*, 11057–11063. [[CrossRef](#)] [[PubMed](#)]
100. Clader, B.D.; Hendrickson, S.M.; Camacho, R.M.; Jacobs, B.C. All-optical microdisk switch using EIT. *Opt. Express* **2013**, *21*, 6169–6179. [[CrossRef](#)] [[PubMed](#)]
101. Kumar, S.; Singh, L. Proposed new approach to design all optical AND gate using plasmonic based Mach-Zehnder interferometer for high speed communication. *Proc. SPIE* **2016**, *9884*, 98842D.
102. Wang, B.; Xiong, L.; Zeng, Q.; Chen, Z.; Lv, H.; Ding, Y.; Du, J.; Yu, H. All-optical Mach-Zehnder interferometer switching based on the phase-shift multiplication effect of an analog on the electromagnetically induced transparency effect. *Opt. Eng.* **2016**, *55*, 067104. [[CrossRef](#)]

103. Piccione, B.; Cho, C.-H.; van Vugt, L.K.; Agarwal, R. All-optical active switching in individual semiconductor nanowires. *Nat. Nanotechnol.* **2012**, *7*, 640. [[CrossRef](#)]
104. Bajcsy, M.; Majumdar, A.; Englund, D.; Vučković, J. Ultra-low power all-optical switching with a single quantum dot in a photonic-crystal cavity. *Proc. SPIE* **2013**, 8635, 863516.
105. Born, B.; Geoffroy-Gagnon, S.; Krupa, J.D.A.; Hristovski, I.R.; Collier, C.M.; Holzman, J.F. Ultrafast all-optical switching via subdiffractive photonic nanojets and select semiconductor nanoparticles. *ACS Photonics* **2016**, *3*, 1095–1101. [[CrossRef](#)]
106. Lu, H.; Liu, X.; Wang, L.; Gong, Y.; Mao, D. Ultrafast all-optical switching in nanoplasmonic waveguide with Kerr nonlinear resonator. *Opt. Express* **2011**, *19*, 2910–2915. [[CrossRef](#)] [[PubMed](#)]
107. Foroutan, S.; Rostami, G.; Dolatyari, M.; Rostami, A. All-optical switching in metal nanoparticles plasmonic waveguide using EIT phenomenon. *Optik* **2017**, *132*, 291–298. [[CrossRef](#)]
108. Neira, A.D.; Wurtz, G.A.; Zayats, A.V. All-optical switching in silicon photonic waveguides with an epsilon-near-zero resonant cavity. *Photon. Res.* **2018**, *6*, B1–B5. [[CrossRef](#)]
109. Nurmohammadi, T.; Abbasian, K.; Yadipour, R. Ultra-fast all-optical plasmon induced transparency in a metal-insulator-metal waveguide containing two Kerr nonlinear ring resonators. *J. Opt.* **2018**, *20*, 055504. [[CrossRef](#)]
110. Kabakova, I.V.; Corcoran, B.; Bolger, J.A.; de Sterke, C.M.; Eggleton, B.J. All-optical self-switching in optimized phase-shifted fiber Bragg grating. *Opt. Express* **2009**, *17*, 5083–5088. [[CrossRef](#)]
111. Zang, Z.; Yang, W. The optical performance of all-optical switching based on fiber Bragg grating. *Proc. SPIE* **2011**, 8040, 80400E.
112. Scholtz, L.; Solanská, M.; Ladányi, L.; Müllerová, J. Power requirements reducing of FBG based all-optical switching. *Proc. SPIE* **2017**, 10603, 1060310.
113. Nozaki, K.; Tanabe, T.; Shinya, A.; Matsuo, S.; Sato, T.; Taniyama, H.; Notomi, M. Sub-femtojoule all-optical switching using a photonic-crystal nanocavity. *Nat. Photonics* **2010**, *4*, 477. [[CrossRef](#)]
114. Ghadrđan, M.; Mansouri-Birjandi, M.A. Low-threshold photonic crystal all-optical switch using plasmonic nanowires placed in nonlinear resonator structure. *J. Nanophoton.* **2017**, *11*, 036017. [[CrossRef](#)]
115. Dawes, A.M.C.; Illing, L.; Clark, S.M.; Gauthier, D.J. All-optical switching in rubidium vapor. *Science* **2005**, *308*, 672–674. [[CrossRef](#)]
116. Huang, Y.; Wu, S.-T.; Zhao, Y. All-optical switching characteristics in bacteriorhodopsin and its applications in integrated optics. *Opt. Express* **2004**, *12*, 895–906. [[CrossRef](#)] [[PubMed](#)]
117. Roy, S.; Sharma, P.; Dharmadhikari, A.K.; Mathur, D. All-optical switching with bacteriorhodopsin. *Opt. Commun.* **2004**, *237*, 251–256. [[CrossRef](#)]
118. Wada, O. Femtosecond all-optical devices for ultrafast communication and signal processing. *New J. Phys.* **2004**, *6*, 183. [[CrossRef](#)]
119. Chai, Z.; Hu, X.; Wang, F.; Niu, X.; Xie, J.; Gong, Q. Ultrafast all-optical switching. *Adv. Opt. Mater.* **2017**, *5*, 1600665. [[CrossRef](#)]
120. Georgiou, K.; Michetti, P.; Gai, L.; Cavazzini, M.; Shen, Z.; Lidzey, D.G. Control over energy transfer between fluorescent BODIPY dyes in a strongly coupled microcavity. *ACS Photonics* **2018**, *5*, 258–266. [[CrossRef](#)]
121. Li, R.; Petit, L.; Franke, D.P.; Dehollain, J.P.; Helsen, J.; Steudtner, M.; Thomas, N.K.; Yoscovits, Z.R.; Singh, K.J.; Wehner, S.; et al. A crossbar network for silicon quantum dot qubits. *Sci. Adv.* **2018**, *4*, eaar3960. [[CrossRef](#)]
122. Paul, N.; Metwalli, E.; Yao, Y.; Schwartzkopf, M.; Yu, S.; Roth, S.V.; Müller-Buschbaum, P.; Paul, A. Templating growth of gold nanostructures with a CdSe quantum dot array. *Nanoscale* **2015**, *7*, 9703–9714. [[CrossRef](#)]

